

Fundamental Insights into Battery Thermal Management and Safety

Ryan S. Longchamps, Xiao-Guang Yang, and Chao-Yang Wang*



Cite This: *ACS Energy Lett.* 2022, 7, 1103–1111



Read Online

ACCESS |



Metrics & More

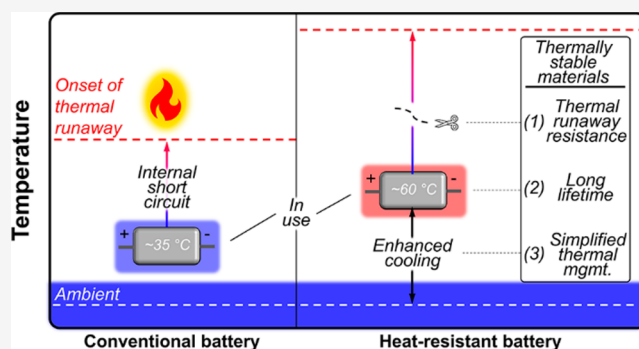


Article Recommendations



Supporting Information

ABSTRACT: To break away from the trilemma among safety, energy density, and lifetime, we present a new perspective on battery thermal management and safety for electric vehicles. We give a quantitative analysis of the fundamental principles governing each and identify high-temperature battery operation and heat-resistant materials as important directions for future battery research and development to improve safety, reduce degradation, and simplify thermal management systems. We find that heat-resistant batteries are indispensable toward resistance to thermal runaway and therefore ultimately battery safety. Concurrently, heat-resistant batteries give rise to long calendar life when idling at ambient temperatures and greatly simplify thermal management while working, owing to much enlarged temperature difference driving cooling. The fundamentals illustrated here reveal an unconventional approach to the development of current and future battery technologies as society moves toward ubiquitous electrified transportation.



To fight against climate change, the burgeoning trend of vehicle electrification is set for continued disruption of the multifaceted, mass-market transportation industry. The slow and arduous process of overhauling such an industry is underway with the lithium-ion battery (LiB) taking a stronghold as the dominant electrochemical engine. With that, the engineering design of battery systems for electric vehicles (EVs) remains dynamic as it trends toward a common understanding of best practices. Battery thermal management (BTM) and safety represent two interdependent and key elements of EV design that remain largely unsolved and ever-evolving.

The critical nature of BTM is rooted in the strong dependence of battery performance, life, and safety on temperature, as illustrated in Figure 1.¹ When operated at an optimal temperature (~ 30 °C), battery life can be maximized by balancing competing degradation mechanisms (e.g., lithium plating at low temperatures and solid–electrolyte interphase (SEI) layer growth at high temperatures).² The challenge in cooling a large number of cells in an EV pack lies in the competition between battery thermal management system (BTMS) weight/volume and cooling capacity. The former affects EV range while the latter, when undersized, provides insufficient cooling and thus, reduced battery life and increased safety concern. This represents one of many unsolved dilemmas in traction battery design that impedes a satisfactory end-user experience.

Battery safety—perhaps more vital to EV adoption—must remain the top priority. If LiBs reach temperatures of ~ 90 – 130 °C via insufficient BTM or other forms of abuse (e.g., short-circuit), the flammability of electrolytes and exothermic decomposition of battery materials introduce the threat of the well-documented and potentially catastrophic failure mode, thermal runaway (TR).^{3–5} The challenge of safe battery operation is also heightened by the trend toward high-voltage ternary layered oxide cathode materials with increasing nickel content, which renders high battery energy density (ED) at the cost of decreased thermal stability.⁶ In the event of overheating, TR mitigation through cooling may be possible, and there is a small temperature range in which cell heat generation does not exceed the cooling capacity of the BTMS (Figure 1). Therefore, the BTMS also provides a barrier against thermal failure.¹ Clearly, key EV metrics (safety, lifetime, range, etc.) compete with each other, and their simultaneous improvement will require battery scientists and engineers to revisit the basics to gain insights that drive stepwise innovation from the materials to system level.

Received: January 11, 2022

Accepted: February 14, 2022

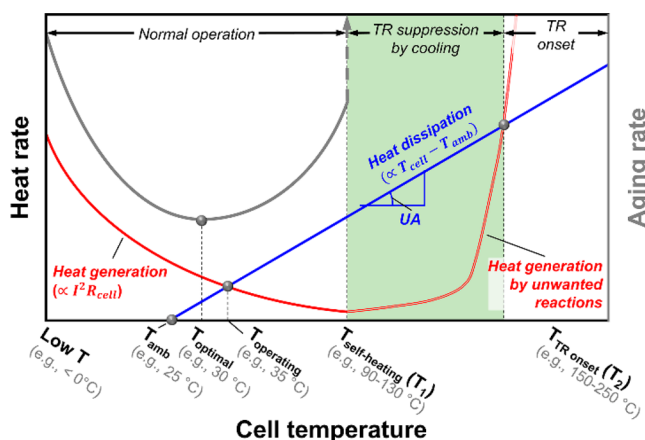


Figure 1. Battery thermal characteristics. The battery thermal management system must dissipate the heat generated during operation to avoid continual temperature rise. Multiple aging mechanisms with varying temperature dependencies result in an optimal operating temperature for battery life, which necessitates temperature regulation by a BTMS. Upon high temperatures resulting from abuse or insufficient cooling, batteries will undergo thermal runaway (TR) via accelerated exothermic reactions between battery materials. The BTMS is a barrier against such thermal failure.

In this Perspective, we relate high-level battery metrics to key process parameters in order to provide a fundamental view of thermal management and safety. The analysis unveils new directions for reinforcing battery safety with a focus on material thermal stability and simplifying thermal management systems through high-temperature battery operation. We then present an example that achieves these two targets by developing heat-resistant battery cells with passive air cooling. Representing a paradigm shift in battery design and operation from the cell to system level, we believe that the new strategies derived herein will enable higher pack-level energy ED, specific energy (SE), and safety for energy-dense battery chemistries of both current and next generations.

BATTERY THERMAL MANAGEMENT

To provide context for the challenge of BTM, the heat generation for various vehicle powertrains (internal combustion engine vehicle (ICEV), fuel cell electric vehicle (FCEV), and battery electric vehicle (BEV)) are compared via eq 1:

$$\dot{q}_{\text{gen}} = P \left(\frac{1}{\eta} - 1 \right) \quad (1)$$

where \dot{q}_{gen} is the rate of heat generated at peak power, P is the peak power (e.g., 100 kW for a passenger vehicle), and η is the system efficiency. We then consider the ideal condition for thermal management, i.e., zero temperature rise, by balancing the heat generation and dissipation rates in eq 2:

$$\dot{q}_{\text{gen}} = UA(T_c - T_{\text{amb}}) \quad (2)$$

where U is the effective heat transfer coefficient between the power system and ambient, A is the effective heat transfer area, T_c is the cell operating temperature, and T_{amb} is the ambient/cooler temperature. The resulting thermal conductance (UA) requirements define the engineering challenge to achieve zero temperature rise, as shown in Table 1. In the case of BEVs, the requisite UA is actually ~ 2.8 times lower than that of the ICEV. Despite this optimistic result, LiB SE is currently limited to 200–300 Wh/kg at the cell level. This necessitates heavy and large battery packs to achieve practical range (200–400 miles), consuming a significant portion of the curb weight (20–30%)⁷ and leaving minimal headroom for parasitic mass associated with battery pack assembly (cables/bus bars, thermal management system, electronics, etc.). In turn, EV manufacturers must innovate to maximize the cell-to-pack conversion efficiency (CTP), defined as the ratio of pack-to-cell SE or ED on a gravimetric (GCTP) or volumetric (VCTP) basis. In a recent survey⁸ of 14 EVs on the market (2017 or later) the average GCTP and VCTP are 0.62 and 0.33, respectively, which fall short of the United States Advanced Battery Consortium (USABC) target for FY2020 of ≥ 0.67 for both GCTP and VCTP.⁹ Looking forward to 2030, the European Council for Automotive R&D (EUCAR) is targeting GCTP and VCTP of 0.8 and 0.75, respectively.¹⁰ The BTMS, generally consuming 5–10% of pack weight,¹¹ presents an opportunity for notable CTP increases. Thus, boosting cell SE and ED while simplifying the BTMS and maintaining safety is a grand challenge for EVs.

To simplify thermal management, we look to eq 2 and identify three opportunities:

- (i) increase the thermal conductance,
- (ii) elevate the cell operating temperature further away from the ambient, i.e., enlarge the temperature difference for cooling, or
- (iii) reduce the heat generation rate (e.g., reduce cell resistance).

Current BTMS designs take inspiration from classical techniques, such as air cooling, direct/indirect liquid cooling, and/or extended heat transfer area (e.g., fins, cold plates, etc.) to increase thermal conductance. In present BTMS designs, surface area for cooling is the limiting factor, but its expansion (e.g., fin arrays) consumes unavailable pack volume.¹⁶ Thus, U must be augmented, which also increases the cost/mass/volume of the overall battery system (pumps, valves, heat exchangers, etc.) along with the parasitic energy consumption for operation. Additionally, the system complexity gives rise to reliability concerns. Thus, while active liquid cooling and, in some cases, air cooling¹⁷ can provide sufficient heat dissipation, it is desirable to seek safer, more reliable, and more efficient approaches to BTM.

Alternatively, passive thermal management is attractive due to the elimination of parasitic power, weight, and space

Table 1. Comparison of Heat Generation and Thermal Management Requirements across Powertrains

powertrain	peak power, P (kW)	efficiency, η (%)	heat generation rate, \dot{q}_{gen} kW	operating temperature, T_c (°C)	$T_c - T_{\text{amb}}$ (°C)	thermal conductance, UA (kW/°C)
ICE		30 ¹²	233	100 ¹³	75	3.1
FC	100	50 ¹⁴	100	80 ¹⁴	55	1.8
LiB		90 ¹⁵	11.1	35 ²	10	1.1

consumption of the auxiliary components of active thermal management. Heat pipes are often labeled as a passive option for BTM.¹ While they are inherently passive on their own and can effectively dissipate heat from the immediate vicinity of cells, the heat must still be transported outside the EV pack, which requires some other auxiliary cooling system. Additionally, their high cost and small contact area remain prohibitive for EV BTM at present.¹⁸ On the other hand, phase change materials (PCMs) could offer a fully passive BTM solution.^{1,19}

PCMs have gained attention in the research community since the proposal of their application to BTM in 2005.²⁰ Effective PCM-based systems have been demonstrated computationally^{20–23} or experimentally at the lab scale;^{20,24,25} however, the practical implications of PCM systems on GCTP and VCTP are rarely reported or discussed. To assess PCMs from a system standpoint, we consider the heat generation of a LiB with a given SE. After accounting for the sensible heat absorbed by both the PCM and cells in raising their temperature from the ambient to operating temperature (assumed approximately equal to average PCM solidus–liquidus temperatures), the GCTP efficiency can be estimated as

$$\text{GCTP} = \frac{\text{SE}_{\text{pack}}}{\text{SE}_{\text{cell}}} = \left(1 + \frac{\text{SE}_{\text{cell}}(1 - \eta) - c_{\text{p,cell}}(T_c - T_{\text{amb}})}{\lambda_{\text{PCM}} + c_{\text{p,PCM}}(T_c - T_{\text{amb}})} + f_{\text{periphery}} \right)^{-1} \quad (3)$$

where SE_i and $c_{\text{p},i}$ are the SE and specific heat of the cell or pack as labeled, λ is the latent heat of fusion for the PCM, and $f_{\text{periphery}}$ is the ratio of periphery mass (cables, pack housing, electronics, etc., excluding the BTMS) to cell mass. Commonly proposed PCMs have a latent heat of fusion of ~ 150 – 250 kJ/kg or 55 Wh/kg on average.^{19,21,24} We conservatively estimate $f_{\text{periphery}}$ as 0.36 (56 and 20% of pack mass come from cells and periphery, respectively), guided by the pack mass breakdown provided by Diekmann et al.²⁶ As shown in Figure 2, the maximum GCTP is 61% and 55% for 200 and 300 Wh/kg cell designs, respectively. Similarly, the VCTP efficiency is estimated as

$$\text{VCTP} = \frac{\text{ED}_{\text{pack}}}{\text{ED}_{\text{cell}}} = \left[1 + \left(\frac{\text{SE}_{\text{cell}}(1 - \eta) - c_{\text{p,cell}}(T_c - T_{\text{amb}})}{\lambda_{\text{PCM}} + c_{\text{p,PCM}}(T_c - T_{\text{amb}})} \right) \left(\frac{\rho_{\text{cell}}}{\rho_{\text{PCM}}} \right) \right]^{-1} \quad (4)$$

where ρ_{cell} and ρ_{PCM} are the pouch cell and PCM densities, respectively. Note the volume of the pack periphery is neglected for a generous estimate. Based on pouch cell and PCM densities of 2000 and 900 kg/m³,^{19,21,24} the VCTP efficiency is 61% and 50% for 400 and 600 Wh/L cells, respectively, meaning that approximately 40–50% of the pack volume would be allocated to PCM material (Figure 2 inset). Therefore, in terms of CTP efficiencies, PCMs offer little or no advantage over current, liquid-cooled EVs. Moreover, the impending adoption of next-generation batteries with SE nearing 500 Wh/kg forecasts even worse CTP efficiencies for PCM-cooled EVs. This, among other limitations (e.g., low thermal conductivity, issues with containing liquefied PCM,

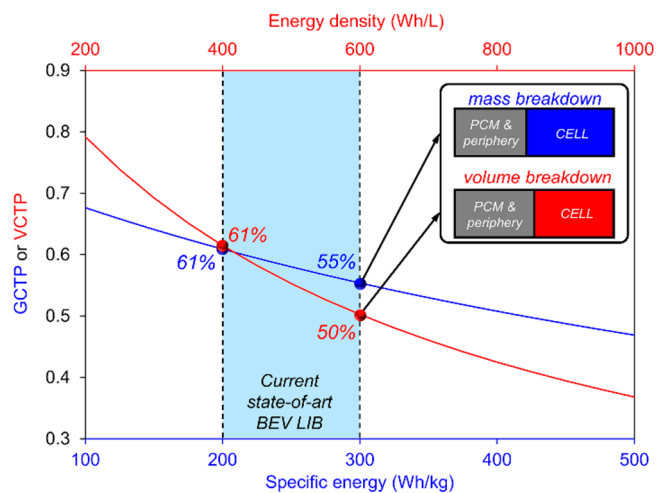


Figure 2. Cell-to-pack assembly efficiencies with PCM. The gravimetric and volumetric cell-to-pack efficiencies vs specific energy (blue) and energy density (red). The inset figure shows the mass and volume break down for a battery pack with 300 Wh/kg cells, the high end of current LIBs. The PCM occupies 45 and 50% of the pack mass and volume to achieve latent heat capacity equivalent to the cell heat generated over one discharge cycle. Note: the results shown correspond to $\eta = 0.9$,¹⁵ $c_{\text{p,cell}} = 1000$ J/kg-K,²⁷ $c_{\text{p,PCM}} = 2000$ J/kg-K,¹⁹ $T_c = 35$ °C, and $T_{\text{amb}} = 25$ °C.

thermal capacity sufficient for only one discharge cycle), renders PCMs unattractive for EV BTM.

Recently, sorbents have been proposed as a near-passive BTM strategy similar to PCMs.¹⁸ Battery heating and cooling occurs via water sorption and desorption, respectively. This technique appears to offer an order-of-magnitude advantage in heat of adsorption over PCMs (~ 220 J/g), owing to the massive heat of vaporization of water (2400 J/g). However, it would be the heat of adsorption per unit mass or volume of sorbents plus water that matters for BTM. It remains to be seen if and how this latter parameter can be made viable for practical application to EV batteries.

Operating batteries at temperatures well above any practical climate eases the thermal conductance requirements to simplify battery thermal management greatly, regardless of ambient conditions.

The shortcomings of previously employed or attempted active and/or passive cooling methods motivate further search for alternative solutions to simplify thermal management, i.e., opportunities in categories (ii) and (iii) described earlier. One bold idea is that if a LiB can be designed similarly to a polymer electrolyte fuel cell operating at 80 °C, opportunities (ii) and (iii) will be fully seized, leading to the virtual disappearance of BTM. This can be readily imagined from Table 1 where a battery operating at 80 °C would have the same temperature difference as a fuel cell to dissipate one tenth of fuel cell heat. Indeed, a class of heat resistant batteries for high safety developed by strong interfacial passivation have recently emerged. These batteries must operate at elevated temperatures, like 60 °C, in order to restore power.^{28,29} Other heat-resistant examples include batteries incorporating an anode

with low Brunauer–Emmett–Teller (BET) area³⁰ paired with a thermally stable LiFePO₄ (LFP) cathode,^{31,32} batteries using LFP-coated high-nickel ternary cathodes,³³ highly concentrated electrolyte³⁴ or ionic liquid batteries,³⁵ and all solid-state batteries.³⁶ These heat-resistant batteries have distinctive advantages in thermal management, as increasing T_c simultaneously augments the temperature difference that drives heat dissipation and exponentially reduces heat generation by lowering cell resistance (Figure 1). The complementary reduction of internal temperature gradients to ensure uniform electrode aging is also afforded, owing to decreased heat flux (due to less heat generation).

We introduce eq 5, which shows $\dot{q}_{\text{gen}} \propto R_{\text{cell}}$, to compare UA requirements for conventional LiBs and heat-resistant batteries

$$UA = \frac{\dot{q}_{\text{gen}}}{(T_c - T_{\text{amb}})} \propto \frac{R_{\text{cell}}}{(T_c - T_{\text{amb}})} \quad (5)$$

operated at, e.g., 60 °C, where R_{cell} is the cell direct-current resistance (DCR) multiplied by the total electrode area for normalization. Based on DCR data from an energy-dense graphite||Li(Ni_{0.8}Co_{0.1}Mn_{0.1})O₂ (NCM811) cell with a conventional electrolyte (~290 Wh/kg),²⁹ Figure 3a shows that

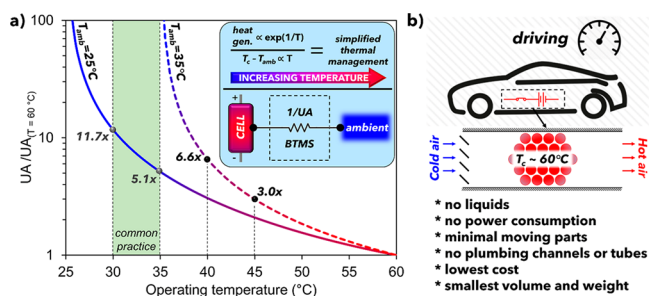


Figure 3. Feasibility of aspirated air cooling for lightweight, low-cost LiB packs. (a) The ratio of cell resistance to ΔT driving heat transfer relative to that at 60 °C for an exemplary high-energy, state-of-the-art LiB.²⁹ The thermal conductance requirements for cooling decreases rapidly by elevating the operating temperature further from the ambient, ultimately reducing the complexity of BTMS. (b) Conceptual thermal management-free, heat-resistant cell implementation in an EV and the benefits to the overall battery pack simplicity, specific energy, and energy density. The relative motion of the vehicle forces cool ambient air over the cell surfaces to dissipate heat and maintain constant cell temperature without parasitic power consumption.

elevating the operating temperature to 60 °C yields a 11.7 and 5.1 times reduction in the UA requirements as compared to 30 and 35 °C operation, respectively (25 °C ambient). Similar advantages exist for operation in regions with hot weather (e.g., 35 °C in Figure 3a), where maintaining battery temperature at 40 or 45 °C is 6.6 and 3.0 times more demanding, respectively, than 60 °C operation. Broadly, operating batteries at temperatures well above any practical climate eases the UA requirements to simplify BTM greatly regardless of ambient conditions.

While BTMS simplification via high operating temperature may come in many forms, we propose a “thermal-management-free” (TMF) EV, as illustrated in Figure 3b. First, two operational strategies for elevating cell temperature exist: one for low power requirements (e.g., city/neighborhood driving) and the other for high-power on demand (e.g., accelerating

onto highways). Both can be chosen on demand. The former consumes no additional energy by allowing the cells to naturally warm up while the latter uses rapid thermal modulation (e.g., 30 s) achieved with intracell heating element(s) (nickel foil(s) in the self-heating battery structure³⁷). The heating energy consumption in the latter case is minimal (<3% for heating from room temperature (RT) to 60 °C), owing to the high efficiency and temperature uniformity of the self-heating structure,³⁸ having a negligible effect on vehicle range. The self-heating structure also offers rapid heating even in ultracold environments (e.g., -40 °C),³⁸ introducing further ambient temperature immunity for EVs. While operating batteries at elevated temperatures as opposed to RT will sacrifice more energy for preheating from such ultracold temperatures, the additional increase (<3%) is negligible compared to the energy unleashed by preheating (i.e., an LiB at <-30 °C can neither discharge any electrical energy at practical rates³⁸ nor recuperate braking energy). Finally, the safety of the self-heating battery structure is ensured by proper engineering and reliability measures that control the heating process, just as in present external battery heating methods for fast-charging and low-temperature operation. In fact, the self-heating structure allows for internal temperature sensing, which can help to bolster safety and provide thermal fault detection.³⁹

Heat-resistant materials and high-temperature operation will be a realistic and important direction for traction battery safety and much simplified or totally eliminated thermal management.

Elevated battery temperature during driving is maintained by balancing the internal heat generation and external heat dissipation, which is controlled by the actuation of louvers that modulate air flow into the moving vehicle (Figure 3b). When heat generation is small and a near-adiabatic condition is required, the louvers are closed. During peak acceleration or at steady, high speeds, the louvers are opened to increase air flow, which is then proportional to vehicle speed.

The feasibility of the TMF design can be determined by comparing the UA capabilities of liquid and aspirated air cooling with the UA requirements for batteries operated at 35 and 60 °C, respectively, as in eq 6:

$$\frac{(UA)_{\text{air}}}{(UA)_{\text{liquid}}} \geq \frac{R_{\text{cell},60^\circ\text{C}} (T_{c,35^\circ\text{C}} - T_{\text{amb}})}{R_{\text{cell},35^\circ\text{C}} (T_{c,60^\circ\text{C}} - T_{\text{amb}})} \quad (6)$$

The right-hand side yields a ratio of 0.20 based on Figure 3 (25 °C ambient), while the ratio of air-to-liquid thermal conductance is approximately 0.33.⁴⁰ Thus, the compounding effects of increased $(T_c - T_{\text{amb}})$ and reduced heat generation outweigh the reduced UA of aspirated air cooling to support TMF feasibility.

The high-level TMF feasibility, solutions for heating to and stable operation at high temperature, and attendant reductions in cost/parasitic mass and volume/parasitic power consumption/system complexity make such a battery system ideally suited for mobile applications such as EVs and electric vertical takeoff and landing (eVTOL) aircraft.^{41,42} Looking further

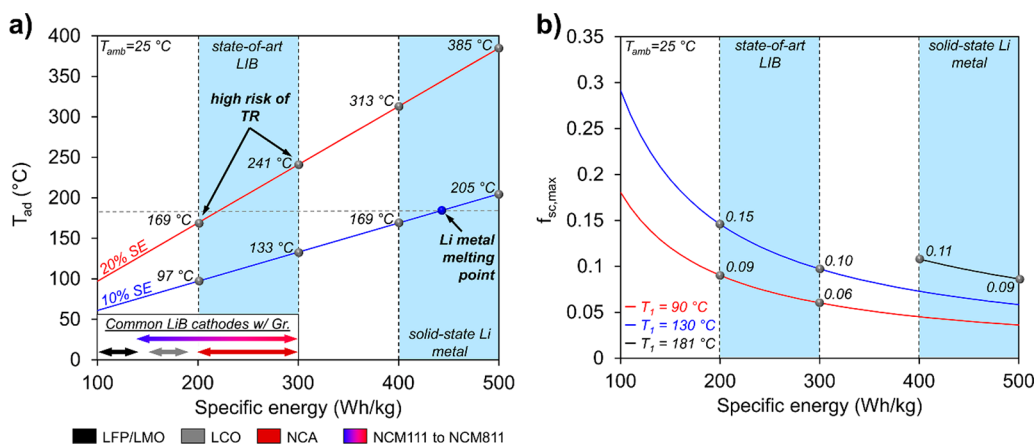


Figure 4. Threat of short-circuit for current and future batteries. (a) The adiabatic temperature achieved by cells of varying specific energy if 10 or 20% of energy is released as heat through short-circuit discharge in 25 °C ambient. SE ranges are shown for common LiB cathodes when paired with a graphite (Gr) anode (LFP/LMO,⁴⁵ LCO,⁴⁵ NCA,⁴⁵ and NCM111⁴⁵ to NCM811²⁹). (b) f_{sc} limits to avoid various self-heating temperatures (T_1) vs cell specific energy.

forward, if a heat-resistant battery can be designed to operate at 80 °C, just like a polymer electrolyte fuel cell, the thermal management system will vanish from the battery pack. Thus, we believe that heat-resistant materials and high-temperature operation will be a realistic and important direction for traction battery safety and much simplified or totally eliminated thermal management.

BATTERY SAFETY

Within the medium temperature range, such as up to 90 °C, the BTMS can serve to prevent TR in conventional LiBs (Figure 1).¹ In general, TR occurs under abuse conditions (e.g., short-circuit, overheating, overcharge, etc.). For current LiBs, once the battery temperature rises beyond ca. 90–130 °C, a cascading sequence of exothermic material decomposition begins. SEI layer thermal decomposition occurs first, enabling exothermic reaction between the anode and electrolyte, which is followed by separator melting, cathode decomposition/oxygen release, and electrolyte decomposition.⁵ Additionally, the low boiling points of pervasive linear carbonate electrolyte solvents (e.g., 91 °C for dimethyl carbonate (DMC) and 110 °C for ethyl methyl carbonate (EMC)) results in a pressure buildup which bursts the cell enclosure at relatively low temperatures, introducing atmospheric oxygen into the cell.⁴³ In the latter phases of the heat-temperature-reaction loop, the temperature skyrockets to ca. 600–1000 °C and violent cell destruction occurs.⁴³ The onset temperature for self-heating is commonly known as T_1 and practically corresponds to the least thermally stable materials within the cell. The temperature when violent TR begins (i.e., “temperature of no return”) is termed T_2 (e.g., 150–250 °C). The vastly detailed nuances of TR are available elsewhere for the interested reader (e.g., ref 3). At a high level, TR prevention requires either complete avoidance of T_1 and/or delay in T_1 and T_2 by increasing the systemic thermal stability of the chosen battery materials.

The TR process summarized above only reflects the chemical nature of a LiB after T_1 has been reached. Here, we have not accounted for heat generation that leads to $T_C \geq T_1$, which usually stems from electrochemical reactions, i.e., the heat that evolves from the inefficiencies of charge/discharge. Note that only the electrochemical nature of a LiB can explain

the strong dependence of TR or battery safety on state of charge, a widely recognized fact. In the event of a short-circuit, the stored electrical battery energy can be fully converted to heat, representing the underlying cause of TR in over 90% of cases.³ It follows that the nominal battery ED should serve as the basis for the threat of TR, as supported by the observations of Lamb et al.⁴⁴ As such, we propose the concept of adiabatic cell temperature (T_{ad}), that is the temperature reached by a cell when all of its discharge energy is released as heat under adiabatic conditions, as expressed in eq 7:

$$q_{gen} = E_{nom} = (It)_{discharge}(U_0 - V_{cell}) = mc_{p,cell}\Delta T_{ad} \quad (7)$$

where q_{gen} is the total heat generation, E_{nom} is the nominal cell energy, $(It)_{discharge}$ is the nominal discharge capacity (current-time product), U_0 is the open-circuit voltage, V_{cell} is the cell voltage (~ 0 V for short-circuit), m is the cell mass, and ΔT_{ad} is the adiabatic temperature rise ($T_{ad} - T_{amb}$). Recasting eq 7 with SE (E_{nom}/m) yields T_{ad} :

$$T_{ad} = \frac{SE}{c_{p,cell}} + T_{amb} \quad (8)$$

Based on $c_{p,cell} = 1000$ J/kg-K,²⁷ 200–300 Wh/kg cells then yield ~ 745 – 1105 °C temperature rise, far exceeding T_1 . We compare the calculation to past experimental results for a 166 Wh/kg, graphite||NCM622 pouch cell, which demonstrated ~ 930 °C temperature rise during nail penetration (NP).²⁸ This corresponds to a total sensible heat gain of 258 Wh/kg (at $c_p = 1000$ J/kg-K), which is ~ 1.6 times the cell electrical energy and confirms the conservative nature of the adiabatic temperature rise based on nominal SE.

It is apparent that only limiting cell electrical energy released through the short-circuit could avoid exceeding T_1 . At only 20% SE release, 200–300 Wh/kg LiBs employing Li($Ni_xCo_yAl_z$)O₂ (NCA)||graphite or Li($Ni_xCo_yMn_z$)O₂ (NCM)||graphite chemistries ($x + y + z = 1$) could reach dangerous temperatures well above T_1 (Figure 4a). The threat to less energy-dense and more thermally stable chemistries, such as LFP||graphite and LiMn₂O₄ (LMO)||graphite, is less severe. Even at only 10% energy release, cells with ca. 300 Wh/kg may be in danger of eventual TR. To explicitly identify safe limits of energy release, we introduce $f_{sc,max}$ which is defined as

the maximum fraction of battery energy allowable before reaching T_1 from T_{amb} under short-circuit, as expressed by

$$f_{\text{sc,max}} = \frac{c_p(T_1 - T_{\text{amb}})}{\text{SE}_{\text{nom}}} \quad (9)$$

For T_1 ranging from 90 to 130 °C, 200 Wh/kg cells can afford 9–15% SE release, while 300 Wh/kg cells must be limited to 6–10% (Figure 4b). Additionally, we build on f_{sc} to define and propose a parameter characterizing NP experiments (T_{NP}^*):

$$T_{\text{NP}}^* = \frac{(T_{\text{max}} - T_{\text{amb}})}{(T_1 - T_{\text{amb}})} \quad (10)$$

where T_{max} is the maximum cell temperature during NP. $T_{\text{NP}}^* < 1$ guarantees safety in the event of short-circuit failure. Note that a valid score relies on an accurate value of T_1 assessed repeatedly through accelerating rate calorimetry (ARC).

Looking beyond Li-ion, all-solid-state batteries (ASSBs) incorporating a solid-state electrolyte with a Li metal anode and high-capacity nickel-rich cathode (e.g., NCM811) are considered the “holy grail” of next-generation, highly safe, energy-dense (e.g., 400–500 Wh/kg) batteries. The elimination of the highly flammable organic liquid electrolytes forms the basis for the claim of ultimate safety. However, a rapid release of only 10% discharge energy of an ASSB could yield temperatures near or above the melting point of Li metal, ~180 °C (Figure 4), indicating the potential for catastrophic failure if molten Li circumvents the electrolyte/separator and making direct contact with the cathode material, a process that is exacerbated by the requisite high clamping pressure applied for electrolyte–electrode interfacial contact (Figure S1; see Supporting Information for ASSB experimental evidence). Thus, the combination of high SE, high charge/discharge (C)-rate operation, and the low melting point of Li metal could pose a severe challenge to the safety of solid-state batteries as the technology evolves, and further restrictions on short-circuit heat release must be required.

The combination of high specific energy, high charge/discharge rate operation, and the low melting point of Li metal could pose a severe challenge to the safety of solid-state batteries as the technology evolves.

Regardless of the chemistry, the safety of current and next-generation EV batteries will benefit from measures of heat absorption and heat dissipation during short-circuit. As discussed earlier, we exclude active cooling and PCMs from consideration given their deleterious impact on CTP efficiencies. One approach that has received popular research attention is to add fire-extinguishing agents (FEAs)⁴⁶ or flame-retardant additives^{47–50} in electrolytes. The most important parameter of FEAs is their endothermic properties, which usually fall between 100 and 200 J/g_{FEA}.⁴⁶ Since LiB chemical energy from combustion significantly exceeds its nominal electrical energy,^{51–53} a generous comparison of FEA and battery mass is made based on the nominal energy of a 200 Wh/kg (720 J/g_{BAT}) LiB. At a minimum, an impractical 3.6 g_{FEA} would be required for every g_{BAT} to stifle or prevent TR. Viability of FEAs for battery safety would thus emerge only

after their endothermic properties can be increased by at least an order of magnitude to 2000 J/g_{FEA} and preferably 2 orders of magnitude.

Rather than designing safety measures to combat TR after it occurs, the safety problem could be solved if a cell design simply lacked the ability to reach TR conditions. To this end, eq 11 offers a roadmap for safe battery design by considering the fundamental dependencies of the rate of temperature rise during a short-circuit event where n is the discharge C-rate:

$$\frac{dT}{dt} \propto \frac{n^* \text{SE}}{c_p} \quad (11)$$

Both C-rate and SE increase the rate of temperature rise and ultimately, the violence of the impending thermal failure, but their reduction for safety purposes sacrifices power performance and range, respectively. Overcoming the power/safety dilemma requires electrochemical interfaces that can activate only when high power is required and deactivate when idling—an impossibility with the conventional LiB structure.

Overcoming the power/safety dilemma requires electrochemical interfaces that can activate only when high power is required and deactivate when idling—an impossibility with the conventional lithium-ion battery structure.

■ A PATH TOWARD BOTH SAFETY AND HIGH ENERGY

A specific example of heat-resistant batteries for both high safety and high ED can be illustrated by a design coined as “safe, energy-dense battery” (SEB).^{28,29} A SEB cell consisted of graphite anodes and NCM811 cathodes with a cathode loading of ~4 mAh/cm², which corresponds to ~290 Wh/kg in a large format cell.²⁹ When a conventional electrolyte (1 M LiPF₆ in ethylene carbonate (EC)/EMC (3:7 wt%) + 2 wt% vinylene carbonate (VC)) is employed and NP is performed, an approximate T_{ad} of 918 °C is expected. This is confirmed by the ~950 °C temperature rise ($T_{\text{NP}}^* = 14.7$ for $T_1 = 85$ °C) in NP tests of the 3.3 Ah experimental cells (Figure 5a). To mitigate this threat, a small amount (e.g., 1.5 wt%) of the flame retardant, triallyl phosphate (TAP), was added to the electrolyte. TAP polymerizes on the cathode and anode during formation to create thick, highly resistive electrode–electrolyte interfaces (EElS),⁵⁴ as the EIS spectra illustrate in Figure 5b. By stifling or “shutting down” electrode reactivity at ambient conditions, the cell response to NP becomes benign. In fact, Figure 5c shows that NP tests of the SEB cells demonstrated extremely slow discharge after penetration and a remarkable T_{NP} of 55 °C, which corresponds to $T_{\text{NP}}^* = 0.52$! The impedance rise attributed to TAP implies poor power performance, but when SEB cells are thermally modulated to 60 °C, the Arrhenius effect “turns on” the EElS to produce a 59% power gain over the baseline at RT. Lastly, the thermal stability and mechanical integrity of the protective EElS—which block lattice oxygen release from the metal oxide cathode, suppress decomposition of organic electrolyte solvents at the cathode and anode, and resist particle fracture/EEl growth during electrode cycling—overcome the

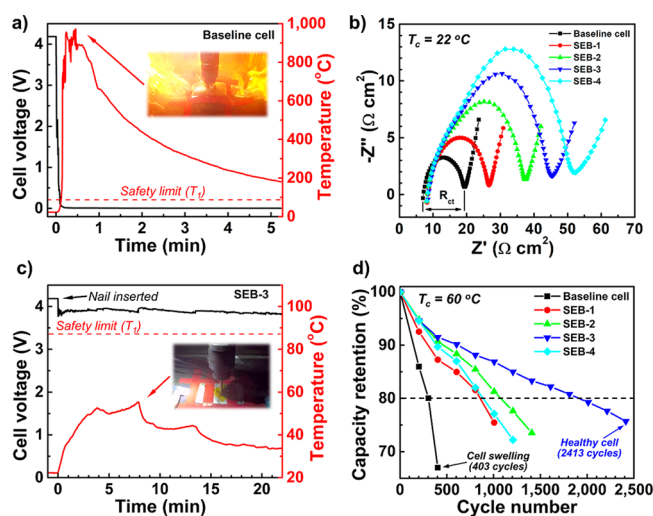


Figure 5. High-temperature stability and safety in a single cell. The baseline electrolyte is 1 M LiPF₆ in ethylene carbonate (EC)/ethyl methyl carbonate (EMC) (3:7 wt%) + 2 wt% vinylene carbonate (VC), while the SEB electrolytes use 1 M LiPF₆ in EC/EMC (1:9 wt%) + 2 wt% VC and varying triallyl phosphate (TAP) contents of 0.5, 1.0, 1.5, and 2.0 wt% for SEB-1, -2, -3, and -4, respectively. (a, c) Temperature and cell voltage evolution during NP testing for the SEB and LiB cells, respectively. (b) EIS spectra for baseline and SEB cells. (d) Capacity retention for baseline and SEB cells cycled at 60 °C. Reprinted with permission from ref 29. Copyright 2021 Elsevier.

issues of cycle life reduction at elevated temperatures in conventional LiBs even in the presence of unstable, high-nickel ternary oxide cathode materials (e.g., SEB-3 in Figure 5d). Moreover, once thermal stability is achieved at elevated temperature of operation (only 5–10% of lifetime), calendar aging at RT is dramatically reduced since RT significantly slows down material degradation and side reactions between the active materials and electrolyte in heat-resistant batteries designed for elevated temperatures. The SEB design, overall, exemplifies the feasibility of the LiB safety and simplified thermal management concepts illustrated in this perspective without the sacrifice of SE/ED. Guided by this example, the door is now open for the battery materials community to discover a vast array of alternative and/or chemistry-specific solutions for heat-resistant design, no longer hindered by the requirement of low impedance at RT.

The door is now open for the battery materials community to discover a vast array of alternative and/or chemistry-specific solutions for heat-resistant design, no longer hindered by the requirement of low impedance at room temperature.

The insights into BTM and safety explored here lead to a redefined schematic of battery thermal characteristics, as shown in Figure 6. Use of thermally stable battery materials can slow aging, enabling long cycle/calendar life while also providing a larger safety barrier between the operating temperature and T_1 , making the target of $T_{NP}^* < 1$ less challenging and effectively eliminating the threat of TR. Also,

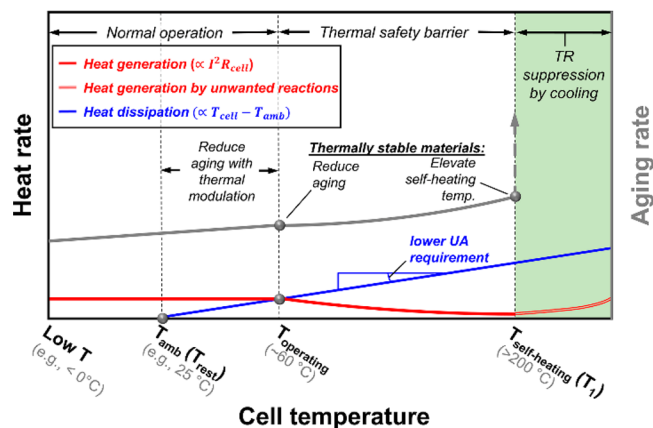


Figure 6. Thermal behavior of heat-resistant batteries built with thermally stable materials and operated at elevated temperature. Thermally stable materials provide safety enhancement and enable long cycle life at all temperatures while agile thermal modulation enables high-power operation. Operation at elevated temperatures also greatly reduces the thermal conductance (UA) requirement of BTMS, simplifying its design and implementation.

thermally stable materials and interfaces enable the battery to operate at high temperatures, significantly enlarging the temperature difference to drive heat dissipation and hence demanding less or no thermal management. The adoption of a self-heating structure permits rapid thermal modulation to the elevated operating temperature for high power regardless of the ambient condition. At storage in equilibrium with the ambient (>~95% of lifetime), the heat-resistant batteries achieve long calendar life while also instilling safety in the event of a short-circuit.

Broadly, for energy-dense LiBs and next-generation batteries (e.g., Li metal ASSB) alike, designing heat-resistant cells for high safety and operating at high temperatures for high power, as displayed in Figure 6, charts a new path to both ultrahigh ED and high safety. Additional gain in pack ED and reduction in cost are also afforded via less or no BTM. These advantages are particularly attractive for light duty, mass-market EVs. Moreover, adopting a bimodal state where batteries are heated upon driving for efficient operation and idle dormant provides a new approach to long lasting EVs that can operate in any practical climate. Lastly, we hope that the approach taken in this Perspective sparks equally unconventional thinking across all areas of battery research to discover unexpected but powerful solutions for the batteries of today and those to come.

■ ASSOCIATED CONTENT

Supporting Information

The Supporting Information is available free of charge at <https://pubs.acs.org/doi/10.1021/acsenergylett.2c00077>.

Additional experimental details, materials, and methods, including photographs of the ARC experimental setup and temperature/voltage evolutions (PDF)

■ AUTHOR INFORMATION

Corresponding Author

Chao-Yang Wang – Electrochemical Engine Center (ECEC) and Department of Mechanical Engineering, The Pennsylvania State University, University Park, Pennsylvania

16802, United States;  orcid.org/0000-0003-0650-0025;
Email: cwx31@psu.edu

Authors

Ryan S. Longchamps – *Electrochemical Engine Center (ECEC) and Department of Mechanical Engineering, The Pennsylvania State University, University Park, Pennsylvania 16802, United States*

Xiao-Guang Yang – *Electrochemical Engine Center (ECEC) and Department of Mechanical Engineering, The Pennsylvania State University, University Park, Pennsylvania 16802, United States;  orcid.org/0000-0002-9880-3682*

Complete contact information is available at:

<https://pubs.acs.org/10.1021/acseenergylett.2c00077>

Notes

The authors declare no competing financial interest.

Biographies

Ryan S. Longchamps received his M.Sc. at the University of Alabama in Huntsville in 2017 and is currently a Ph.D. candidate working in the Electrochemical Engine Center at the Pennsylvania State University. His research mainly focuses on battery thermal management and safety as well as novel battery structures.

Xiao-Guang Yang (Ph.D., Mechanical Engineering, Shanghai Jiao Tong University, 2014) served as a postdoc (2014–2018) and Assistant Research Professor (2014–2018) at the Pennsylvania State University. He is currently a Professor at Beijing Institute of Technology, focusing on modeling/diagnostics of heat/mass transfer in electrochemical energy systems.

Chao-Yang Wang is the William E. Diefenderfer Chair Professor of Mechanical Engineering and Professor of Chemical Engineering and Materials Science & Engineering at the Pennsylvania State University. His research covers the transport, materials, manufacturing, and modeling of batteries and fuel cells.

REFERENCES

- (1) Lin, J.; Liu, X.; Li, S.; Zhang, C.; Yang, S. A Review on Recent Progress, Challenges and Perspective of Battery Thermal Management System. *Int. J. Heat Mass Transfer* **2021**, *167*, 120834.
- (2) Yang, X.-G.; Wang, C.-Y. Understanding the Trilemma of Fast Charging, Energy Density and Cycle Life of Lithium-Ion Batteries. *J. Power Sources* **2018**, *402*, 489–498.
- (3) Feng, X.; Ren, D.; He, X.; Ouyang, M. Mitigating Thermal Runaway of Lithium-Ion Batteries. *Joule* **2020**, *4* (4), 743–770.
- (4) Huang, W.; Feng, X.; Han, X.; Zhang, W.; Jiang, F. Questions and Answers Relating to Lithium-Ion Battery Safety Issues. *Cell Reports Physical Science* **2021**, *2* (1), 100285.
- (5) Feng, X.; Ouyang, M.; Liu, X.; Lu, L.; Xia, Y.; He, X. Thermal Runaway Mechanism of Lithium Ion Battery for Electric Vehicles: A Review. *Energy Storage Materials* **2018**, *10*, 246–267.
- (6) Bak, S.-M.; Hu, E.; Zhou, Y.; Yu, X.; Senanayake, S. D.; Cho, S.-J.; Kim, K.-B.; Chung, K. Y.; Yang, X.-Q.; Nam, K.-W. Structural Changes and Thermal Stability of Charged $\text{LiNi}_x\text{Mn}_y\text{Co}_z\text{O}_2$ Cathode Materials Studied by Combined In Situ Time-Resolved XRD and Mass Spectroscopy. *ACS Appl. Mater. Interfaces* **2014**, *6* (24), 22594–22601.
- (7) Masias, A. Lithium Ion Battery Design for Transportation. In *Behavior of Lithium-Ion Batteries in Electric Vehicles: Battery Health, Performance, Safety, and Cost*; Pistoia, G., Liaw, B., Eds.; Springer International Publishing, 2018; pp 1–34.
- (8) Yang, X.-G.; Liu, T.; Wang, C.-Y. Thermally Modulated Lithium Iron Phosphate Batteries for Mass-Market Electric Vehicles. *Nature Energy* **2021**, *6* (2), 176–185.
- (9) Christophersen, J. P. *Battery Test Manual For Electric Vehicles, Revision 3*, Report INL/EXT-15-34184; Idaho National Laboratory, June 1, 2015. DOI: 10.2172/1186745
- (10) Battery Requirements for Future Automotive Applications; European Council for Automotive R&D, July 2019; <https://eucar.be/wp-content/uploads/2019/08/20190710-EG-BEV-FCEV-Battery-requirements-FINAL.pdf>.
- (11) Nelson, P. A.; Ahmed, S.; Gallagher, K. G.; Dees, D. W. *Modeling the Performance and Cost of Lithium-Ion Batteries for Electric-Drive Vehicles*, 3rd ed., Report ANL/CSE-19/2; Argonne National Laboratory, March 1, 2019. DOI: 10.2172/1503280
- (12) Boretto, A. A. Energy Recovery in Passenger Cars. *J. Energy Resour. Technol.* **2012**, *134* (2), 022203–022210.
- (13) Roberts, A.; Brooks, R.; Shipway, P. Internal Combustion Engine Cold-Start Efficiency: A Review of the Problem, Causes and Potential Solutions. *Energy Conversion and Management* **2014**, *82*, 327–350.
- (14) Shen, P. K.; Wang, C. Y.; Jiang, S. P.; Sun, X.; Zhang, J. Introduction to Electrochemical Energy Storage and Conversion. *Electrochemical Energy: Advanced Materials and Technologies*; CRC Press: Boca Raton, FL, 2016; pp 3–32.
- (15) Meister, P.; Jia, H.; Li, J.; Kloepsch, R.; Winter, M.; Placke, T. Best Practice: Performance and Cost Evaluation of Lithium Ion Battery Active Materials with Special Emphasis on Energy Efficiency. *Chem. Mater.* **2016**, *28* (20), 7203–7217.
- (16) Masias, A.; Marcicki, J.; Paxton, W. A. Opportunities and Challenges of Lithium Ion Batteries in Automotive Applications. *ACS Energy Lett.* **2021**, *6* (2), 621–630.
- (17) Offer, G.; Patel, Y.; Hales, A.; Diaz, L. B.; Marzook, M. Cool Metric for Lithium-Ion Batteries Could Spur Progress. *Nature* **2020**, *582* (7813), 485–487.
- (18) Xu, J.; Chao, J.; Li, T.; Yan, T.; Wu, S.; Wu, M.; Zhao, B.; Wang, R. Near-Zero-Energy Smart Battery Thermal Management Enabled by Sorption Energy Harvesting from Air. *ACS Cent. Sci.* **2020**, *6* (9), 1542–1554.
- (19) Chen, J.; Kang, S.; E, J.; Huang, Z.; Wei, K.; Zhang, B.; Zhu, H.; Deng, Y.; Zhang, F.; Liao, G. Effects of Different Phase Change Material Thermal Management Strategies on the Cooling Performance of the Power Lithium Ion Batteries: A Review. *J. Power Sources* **2019**, *442*, 227228.
- (20) Mills, A.; Al-Hallaj, S. Simulation of Passive Thermal Management System for Lithium-Ion Battery Packs. *J. Power Sources* **2005**, *141* (2), 307–315.
- (21) Sabbah, R.; Kizilel, R.; Selman, J. R.; Al-Hallaj, S. Active (Air-Cooled) vs. Passive (Phase Change Material) Thermal Management of High Power Lithium-Ion Packs: Limitation of Temperature Rise and Uniformity of Temperature Distribution. *J. Power Sources* **2008**, *182* (2), 630–638.
- (22) Fathabadi, H. A Novel Design Including Cooling Media for Lithium-Ion Batteries Pack Used in Hybrid and Electric Vehicles. *J. Power Sources* **2014**, *245*, 495–500.
- (23) Verma, A.; Shashidhara, S.; Rakshit, D. A Comparative Study on Battery Thermal Management Using Phase Change Material (PCM). *Thermal Science and Engineering Progress* **2019**, *11*, 74–83.
- (24) Goli, P.; Legedza, S.; Dhar, A.; Salgado, R.; Renteria, J.; Balandin, A. A. Graphene-Enhanced Hybrid Phase Change Materials for Thermal Management of Li-Ion Batteries. *J. Power Sources* **2014**, *248*, 37–43.
- (25) Weng, J.; Yang, X.; Zhang, G.; Ouyang, D.; Chen, M.; Wang, J. Optimization of the Detailed Factors in a Phase-Change-Material Module for Battery Thermal Management. *Int. J. Heat Mass Transfer* **2019**, *138*, 126–134.
- (26) Diekmann, J.; Hanisch, C.; Froböse, L.; Schällicke, G.; Loellhoeffel, T.; Fölster, A.-S.; Kwade, A. Ecological Recycling of Lithium-Ion Batteries from Electric Vehicles with Focus on Mechanical Processes. *J. Electrochem. Soc.* **2017**, *164* (1), A6184.
- (27) Zhang, X.; Klein, R.; Subbaraman, A.; Chumakov, S.; Li, X.; Christensen, J.; Linder, C.; Kim, S. U. Evaluation of Convective Heat Transfer Coefficient and Specific Heat Capacity of a Lithium-Ion

Battery Using Infrared Camera and Lumped Capacitance Method. *J. Power Sources* **2019**, *412*, 552–558.

(28) Ge, S.; Leng, Y.; Liu, T.; Longchamps, R. S.; Yang, X.-G.; Gao, Y.; Wang, D.; Wang, D.; Wang, C.-Y. A New Approach to Both High Safety and High Performance of Lithium-Ion Batteries. *Science Advances* **2020**, *6* (9), eaay7633.

(29) Ge, S.; Longchamps, R. S.; Liu, T.; Liao, J.; Leng, Y.; Wang, C.-Y. High Safety and Cycling Stability of Ultrahigh Energy Lithium Ion Batteries. *Cell Reports Physical Science* **2021**, *2* (10), 100584.

(30) Agubra, V.; Fergus, J. Lithium Ion Battery Anode Aging Mechanisms. *Materials* **2013**, *6* (4), 1310–1325.

(31) Kassem, M.; Bernard, J.; Revel, R.; Pélissier, S.; Duclaud, F.; Delacourt, C. Calendar Aging of a Graphite/LiFePO₄ Cell. *J. Power Sources* **2012**, *208*, 296–305.

(32) Han, X.; Ouyang, M.; Lu, L.; Li, J.; Zheng, Y.; Li, Z. A Comparative Study of Commercial Lithium Ion Battery Cycle Life in Electrical Vehicle: Aging Mechanism Identification. *J. Power Sources* **2014**, *251*, 38–54.

(33) Chen, J.; Zhu, L.; Jia, D.; Jiang, X.; Wu, Y.; Hao, Q.; Xia, X.; Ouyang, Y.; Peng, L.; Tang, W.; Liu, T. LiNi_{0.8}Co_{0.15}Al_{0.05}O₂ Cathodes Exhibiting Improved Capacity Retention and Thermal Stability Due to a Lithium Ion Phosphate Coating. *Electrochim. Acta* **2019**, *312*, 179–187.

(34) Leng, Y.; Ge, S.; Yang, X.-G.; Longchamps, R. S.; Liu, T.; Wang, C.-Y. Fast Charging of Energy-Dense Lithium Metal Batteries in Localized Ether-Based Highly Concentrated Electrolytes. *J. Electrochem. Soc.* **2021**, *168* (6), 060548.

(35) Plylahan, N.; Kerner, M.; Lim, D.-H.; Matic, A.; Johansson, P. Ionic Liquid and Hybrid Ionic Liquid/Organic Electrolytes for High Temperature Lithium-Ion Battery Application. *Electrochim. Acta* **2016**, *216*, 24–34.

(36) Du, F.; Zhao, N.; Li, Y.; Chen, C.; Liu, Z.; Guo, X. All Solid State Lithium Batteries Based on Lamellar Garnet-Type Ceramic Electrolytes. *J. Power Sources* **2015**, *300*, 24–28.

(37) Wang, C.-Y.; Zhang, G.; Ge, S.; Xu, T.; Ji, Y.; Yang, X.-G.; Leng, Y. Lithium-Ion Battery Structure That Self-Heats at Low Temperatures. *Nature, London* **2016**, *529* (7587), 515–518E.

(38) Longchamps, R. S.; Yang, X.-G.; Ge, S.; Liu, T.; Wang, C.-Y. Transforming Rate Capability through Self-Heating of Energy-Dense and Next-Generation Batteries. *J. Power Sources* **2021**, *510*, 230416.

(39) Zhang, G.; Ge, S.; Xu, T.; Yang, X.-G.; Tian, H.; Wang, C.-Y. Rapid Self-Heating and Internal Temperature Sensing of Lithium-Ion Batteries at Low Temperatures. *Electrochim. Acta* **2016**, *218*, 149–155.

(40) Han, T.; Khalighi, B.; Yen, E. C.; Kaushik, S. Li-Ion Battery Pack Thermal Management: Liquid Versus Air Cooling. *Journal of Thermal Science and Engineering Applications* **2019**, *11*, 021009.

(41) Fredericks, W. L.; Sripad, S.; Bower, G. C.; Viswanathan, V. Performance Metrics Required of Next-Generation Batteries to Electrify Vertical Takeoff and Landing (VTOL) Aircraft. *ACS Energy Lett.* **2018**, *3* (12), 2989–2994.

(42) Yang, X.-G.; Liu, T.; Ge, S.; Rountree, E.; Wang, C.-Y. Challenges and Key Requirements of Batteries for Electric Vertical Takeoff and Landing Aircraft. *Joule* **2021**, *5* (7), 1644–1659.

(43) Feng, X.; Zheng, S.; He, X.; Wang, L.; Wang, Y.; Ren, D.; Ouyang, M. Time Sequence Map for Interpreting the Thermal Runaway Mechanism of Lithium-Ion Batteries With LiNi_xCo_yMn_zO₂ Cathode. *Front. Energy Res.* **2018**, *6*, 126.

(44) Lamb, J.; Torres-Castro, L.; Hewson, J. C.; Shurtz, R. C.; Preger, Y. Investigating the Role of Energy Density in Thermal Runaway of Lithium-Ion Batteries with Accelerating Rate Calorimetry. *J. Electrochem. Soc.* **2021**, *168* (6), 060516.

(45) Zubi, G.; Dufo-López, R.; Carvalho, M.; Pasaoglu, G. The Lithium-Ion Battery: State of the Art and Future Perspectives. *Renewable and Sustainable Energy Reviews* **2018**, *89*, 292–308.

(46) Yim, T.; Park, M.-S.; Woo, S.-G.; Kwon, H.-K.; Yoo, J.-K.; Jung, Y. S.; Kim, K. J.; Yu, J.-S.; Kim, Y.-J. Self-Extinguishing Lithium Ion Batteries Based on Internally Embedded Fire-Extinguishing Micro-

capsules with Temperature-Responsiveness. *Nano Lett.* **2015**, *15* (8), 5059–5067.

(47) Hyung, Y. E.; Vissers, D. R.; Amine, K. Flame-Retardant Additives for Lithium-Ion Batteries. *J. Power Sources* **2003**, *119–121*, 383–387.

(48) Liu, K.; Liu, W.; Qiu, Y.; Kong, B.; Sun, Y.; Chen, Z.; Zhuo, D.; Lin, D.; Cui, Y. Electrospun Core-Shell Microfiber Separator with Thermal-Triggered Flame-Retardant Properties for Lithium-Ion Batteries. *Science Advances* **2017**, *3* (1), e1601978.

(49) Wang, Q.; Sun, J.; Yao, X.; Chen, C. 4-Isopropyl Phenyl Diphenyl Phosphate as Flame-Retardant Additive for Lithium-Ion Battery Electrolyte. *Electrochem. Solid-State Lett.* **2005**, *8* (9), A467.

(50) Shim, E.-G.; Nam, T.-H.; Kim, J.-G.; Kim, H.-S.; Moon, S.-I. Electrochemical Performance of Lithium-Ion Batteries with Triphenylphosphate as a Flame-Retardant Additive. *J. Power Sources* **2007**, *172* (2), 919–924.

(51) Ribière, P.; Grugeon, S.; Morcrette, M.; Boyanov, S.; Laruelle, S.; Marlair, G. Investigation on the Fire-Induced Hazards of Li-Ion Battery Cells by Fire Calorimetry. *Energy Environ. Sci.* **2012**, *5* (1), 5271–5280.

(52) Liu, X.; Stolarov, S. I.; Denlinger, M.; Masias, A.; Snyder, K. Comprehensive Calorimetry of the Thermally-Induced Failure of a Lithium Ion Battery. *J. Power Sources* **2015**, *280*, 516–525.

(53) Ping, P.; Wang, Q.; Huang, P.; Li, K.; Sun, J.; Kong, D.; Chen, C. Study of the Fire Behavior of High-Energy Lithium-Ion Batteries with Full-Scale Burning Test. *J. Power Sources* **2015**, *285*, 80–89.

(54) Xia, J.; Madec, L.; Ma, L.; Ellis, L. D.; Qiu, W.; Nelson, K. J.; Lu, Z.; Dahn, J. R. Study of Triallyl Phosphate as an Electrolyte Additive for High Voltage Lithium-Ion Cells. *J. Power Sources* **2015**, *295*, 203–211.

JACS Au
AN OPEN ACCESS JOURNAL OF THE AMERICAN CHEMICAL SOCIETY

Editor-in-Chief
Prof. Christopher W. Jones
Georgia Institute of Technology, USA

Open for Submissions

ACS Publications
Most Trusted. Most Cited. Most Read.
pubs.acs.org/jacsau